

# Experimental Investigations on Solid State LPG Sensor Using $\text{ZnFe}_2\text{O}_4$ Nanocomposite Prepared by Co-Precipitation Method

Anuradha Yadav<sup>\*1</sup> and B. C. Yadav<sup>2</sup>

1. Nanomaterials and Sensors Research Laboratory, Department of Physics, University of Lucknow, Lucknow-226007, U.P., India

2. Department of Applied Physics, School for Physical Sciences, Babasaheb Bhimrao Ambedkar University, Lucknow-226025, U.P., India

**Abstract:** Zinc ferrite nanocomposite was synthesized via co-precipitation method and their electrical and liquefied petroleum gas sensing were investigated. The structural and morphological characterizations of the sensing material were analyzed by means of XRD (X-ray diffraction) and SEM (Scanning electron microscopy). XRD pattern revealed crystalline and cubic crystal structure. SEM images show spherical nanoparticles distributed throughout the surface. Optical properties were investigated by using UV (Ultraviolet)-visible absorption spectroscopy and FTIR (Fourier transform infrared spectroscopy) techniques. Solid state pellet was investigated with the exposition of LPG (Liquefied petroleum gas). Variations in resistance with time for different concentrations of LPG were recorded at room temperature. The maximum value of sensitivity and sensor response were found 6 and 496 respectively.

**Key words:** Zinc ferrite, nanocomposite, LPG (Liquefied petroleum gas) sensor, pellet, SEM (Scanning electron microscopy), XRD (X-ray diffraction), UV (Ultraviolet), FTIR (Fourier transform infrared spectroscopy).

## 1. Introduction

Chemical sensors play a very important role in both environmental protection and human health. The fabrication of metal oxide semiconducting nanomaterials with large surface to volume ratio for gas sensing applications is currently a major hub of nanoscience and nanotechnology [1]. In recent years, the synthesis of nanocrystalline metal oxide materials has been a focal point of research and developmental activities in the area of nanomaterials owing to the quest for their various technological applications [2-5]. Semiconducting metal oxides such as  $\text{SnO}_2$  [6],  $\text{ZnO}$  [7],  $\text{WO}_3$  [8] and  $\text{Fe}_2\text{O}_3$  [9] have been widely used as gas sensing materials for the detection of the inflammable and toxic gases. The sensor performance strongly dependent on the microstructural features such as crystallite size, grain boundary characteristics

and thermal stability. Several approaches have been explored to fabricate the sensors with improved performance, which includes nano sized crystallites, solid solutions and additives or surface functionalization [10, 11].

Recently, some composite oxides such as spinel  $\text{AB}_2\text{O}_4$  [12] and perovskite  $\text{ABO}_3$  [13] were found to be more attractive than single-metal oxides for their better selectivity and/or sensitivity to certain gases. In particular, the spinel-structured  $\text{ZnFe}_2\text{O}_4$ , in which the transition metal cation  $\text{Zn}^{++}$  was incorporated into the lattice of the parent structure of  $(\text{Fe}^{2+}\text{Fe}_2^{3+}\text{O}_4)$ , was established to be a promising material in detecting reducing gases [14]. Other earlier reports about the application study of zinc ferrite as a gas sensing material include  $\text{ZnFe}_2\text{O}_4$  particles to  $\text{H}_2\text{S}$  [15], a directly deposited film to  $\text{CO}$  [16], ultrafine powder to  $\text{Cl}_2$  [17],  $\text{CdO}$ -doped  $\text{ZnFe}_2\text{O}_4$  to ethanol [18], a  $\text{ZnO}/\text{ZnFe}_2\text{O}_4$  thick film to propanol [19], and so on.

In spite of extensive research on  $\text{ZnFe}_2\text{O}_4$  gas

<sup>\*</sup>**Corresponding author:** Anuradha Yadav, Ph.D., research fields: synthesis and characterization of nanomaterials.

sensors using various sensor systems, target gas, and the fundamental understanding of the sensing properties of the metal oxides is still poor since the focus has been on the empirical optimization of sensor performance. In this work, we have focused on the synthesis and characterization of  $\text{ZnFe}_2\text{O}_4$  via co-precipitation method to enhance the surface area and minimize the crystal size so that the sensitivity would become higher as comparable to earlier reports. With the objective to search for new sensing material for the detection of LPG at room temperature, I have made an attempt to synthesize zinc ferrite nanocomposite by co-precipitation method and to investigate the response of LPG and other reducing gases on it.

## 2. Experimental

### 2.1 Synthesis of Material

Zinc chloride and Ferric chloride solutions were made by dissolving required amount of their salts in de-ionized water to form 1.0 M solution. The nano powder used for the preparation of pellet was made by chemical mixing of  $\text{ZnCl}_2$  and  $\text{FeCl}_3$  solutions and then precipitation by a drop wise addition of base agent e.g., ammonium hydroxide ( $\text{NH}_4\text{OH}$ ). Small amount (5-10 ml) of ethylene glycol was added as capping reagent. Vigorous stirring was done for 18-24 h to ensure complete and intimate reaction between the various components. The product was dried 5-8 h at  $80^\circ\text{C}$  in an oven and calcined at  $400^\circ\text{C}$  for 3 h, resulting at complete crystallization in to powder form.

### 2.2 Preparation of Sensing Pellet

Synthesized powder was grind with mortar and paste for 6 h. The material was subjected to polarization using hydraulic press at an uniaxial pressure 615 MPa at room temperature. The dimension of pellet was 10 mm in diameter and 4 mm in thickness. This pellet was heat treated in an electric furnace (Ambassador, India) at  $550^\circ\text{C}$  for 3 h in the

presence of 20% oxygen and after annealing it was exposed to liquefied petroleum gas in specially designed gas chamber at controlled conditions.

### 2.3 Gas Sensing Measurements

Synthesized pellet was exposed to liquefied petroleum gas in specially designed gas chamber at controlled conditions. Experimental set-up consist two parts; one part shown in Fig. 1a for the measurement of volume of gas and other part shown in Fig. 1b for LPG sensing. Pellet was inserted between the Ag electrodes and gas was introduced through inlet and released from outlet. Corresponding variations in resistance were recorded with Keithley Electrometer.

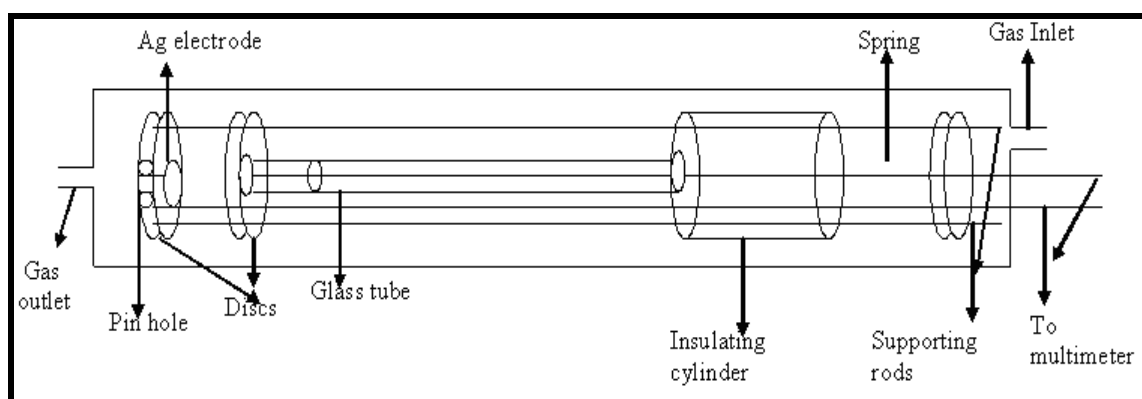
### 2.4 Electrical Measurements in Air (*R-T Characteristic*)

For measuring the electrical properties of sensing elements in air, the sensing elements were put inside a tubular furnace at the highest point of temperature profile with electrical connections and variations in electrical resistance with temperature were recorded. The used heating rate was  $2^\circ\text{C}$  per minute. The temperature dependent resistance measurement shows the thermally activated exponential behaviour of zinc ferrite.

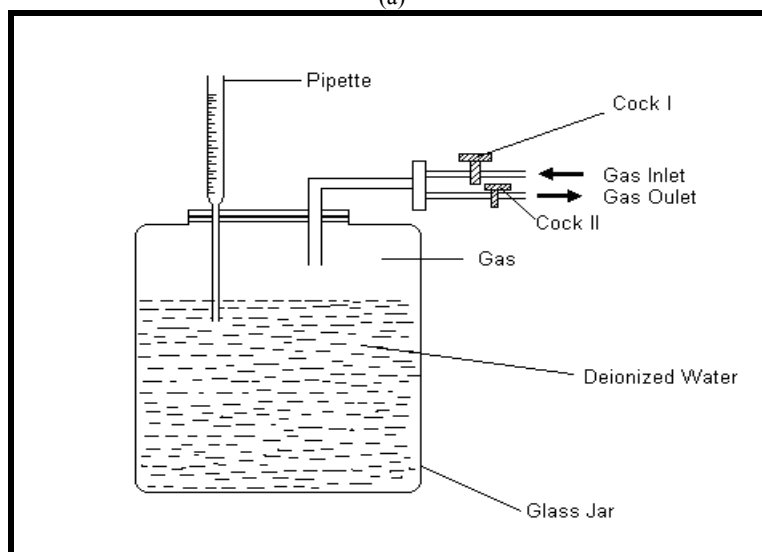
## 3. Characterizations

### 3.1 X-ray Diffraction

The crystal structure and phase of the powdered material was analyzed using X-ray Diffractometer (X-Pert, PRO PANalytical XRD system, Nether land) with  $\text{Cu K}_\alpha$  radiations as source having wavelength  $1.5418 \text{ \AA}$ . XRD pattern of the synthesized powder shown in Fig. 2 reveals the formation of  $\text{ZnFe}_2\text{O}_4$ . Miller indices [h k l] for each oxide are indicated on each of the diffraction peaks.  $\text{ZnFe}_2\text{O}_4$  exists in majority which have rhombohedral crystal system with lattice constants  $a = 5.0787\text{\AA}$ ,  $b = 5.0787\text{\AA}$ ,  $c = 13.927\text{\AA}$ ;  $\alpha = \beta = 90^\circ$ ,  $\gamma = 120^\circ$ . It contains major phase of  $\text{ZnFe}_2\text{O}_4$  at the plane (311) for  $2\theta = 35.61^\circ$ .



(a)



(b)

Fig. 1 (a) Device assembly for measurement of volume of gas, (b) device assembly for measurement.

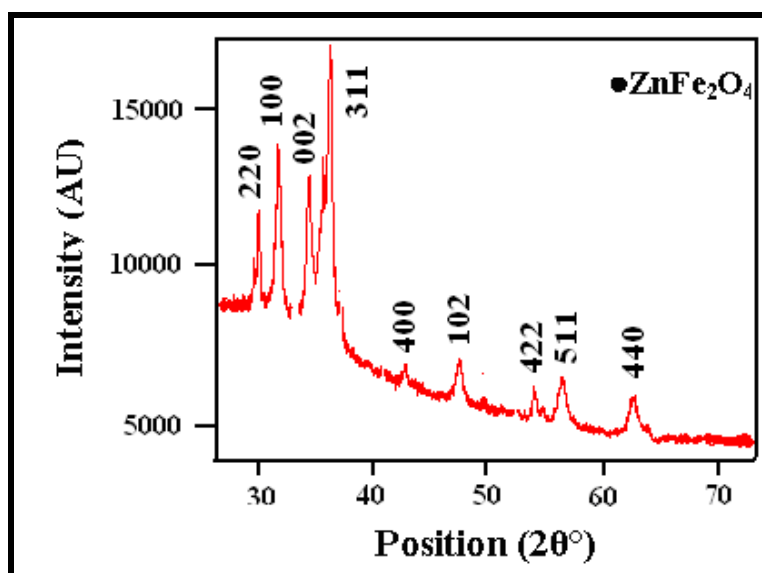


Fig. 2 X-ray diffraction pattern of  $\text{ZnFe}_2\text{O}_4$  nanocomposite.

The FWHM and d-spacing corresponding to this peak are 1.5° and 2.5195 Å respectively. By using Debye-Scherrer formula [20], minimum crystallite size was found 8 nm.

### 3.2 Surface Morphology

The morphology of the sensing surface of pellet before exposition of LPG can be visualized from the Scanning electron microscope (SEM, LEO-0430 Cambridge) as shown in Fig. 3 a. It shows that some of the nanoparticles of the ZnFe<sub>2</sub>O<sub>4</sub> combined with each other to form clusters and leaving some spaces as pores. These pores serve as gas adsorption sites and gas sensitivity depends on the size of these pores. These adsorption sites are disappeared after the adsorption of LPG on the surface of the sensing film as shown in Fig. 2b.

### 3.3 UV-Visible Absorption Analysis

Optical characterization of the sensing material was done by using UV-Visible spectrophotometer (Varian, Carry-50Bio). Fig. 7a shows the absorption spectra of the zinc oxide in the photon energy range 1.112 to 6.19 eV (i.e. 300-1000 nm). One of the sensing materials coated on the borosilicate glass substrate was used for this purpose. Fig. 7 shows that

absorbance decreases with increase in wavelength. In the UV region i.e. approximately in the range 4.0-3.5 eV, curves show steep decrease in absorbance. The relation between absorption coefficient and photon energy is given below:

$$\alpha(E) \propto (E - E_g)^n \quad (1)$$

where, E is the photon energy and E<sub>g</sub> is the optical band gap energy of the material. The above equation shows a linear dependence of (αhν)<sup>2</sup> on photon energy (hν). Figs. 4a and 4b show UV-visible absorption spectra of zinc ferrite nanocomposite in UV and visible range. Zinc ferrite nanoparticles exhibit a strong change of their optical absorption when their size is reduced down to a few nanometers. Therefore, absorption spectra of zinc ferrite nanoparticles obtained in the UV-visible region show blue shift in the absorption edge. The corresponding band gap was 3.9 eV.

### 3.4 FTIR Analysis

The FT-IR analysis was carried out under O<sub>2</sub>/He gas at room temperature. IR spectra were obtained by pressing the zinc ferrite powder by hydraulic press in to pellet form. Fig. 5 shows the FTIR spectra of synthesized ZnFe<sub>2</sub>O<sub>4</sub>. Here, the band at 594 cm<sup>-1</sup> is

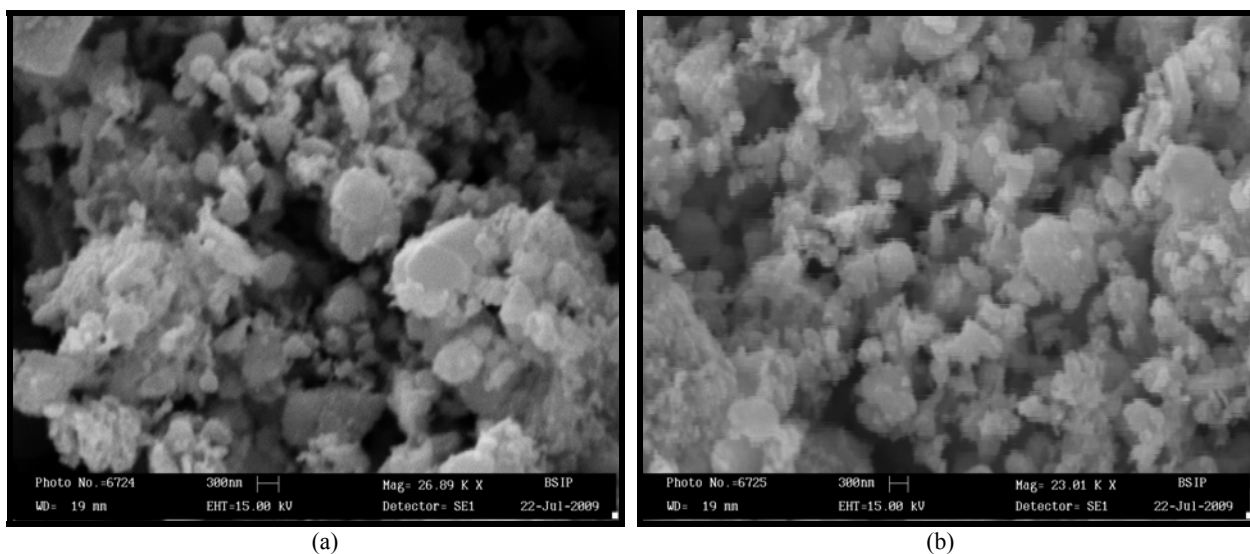


**Fig. 3 (a) Scanning electron micrograph of ZnFe<sub>2</sub>O<sub>4</sub> before exposure to LPG, (b) after exposure to LPG.**

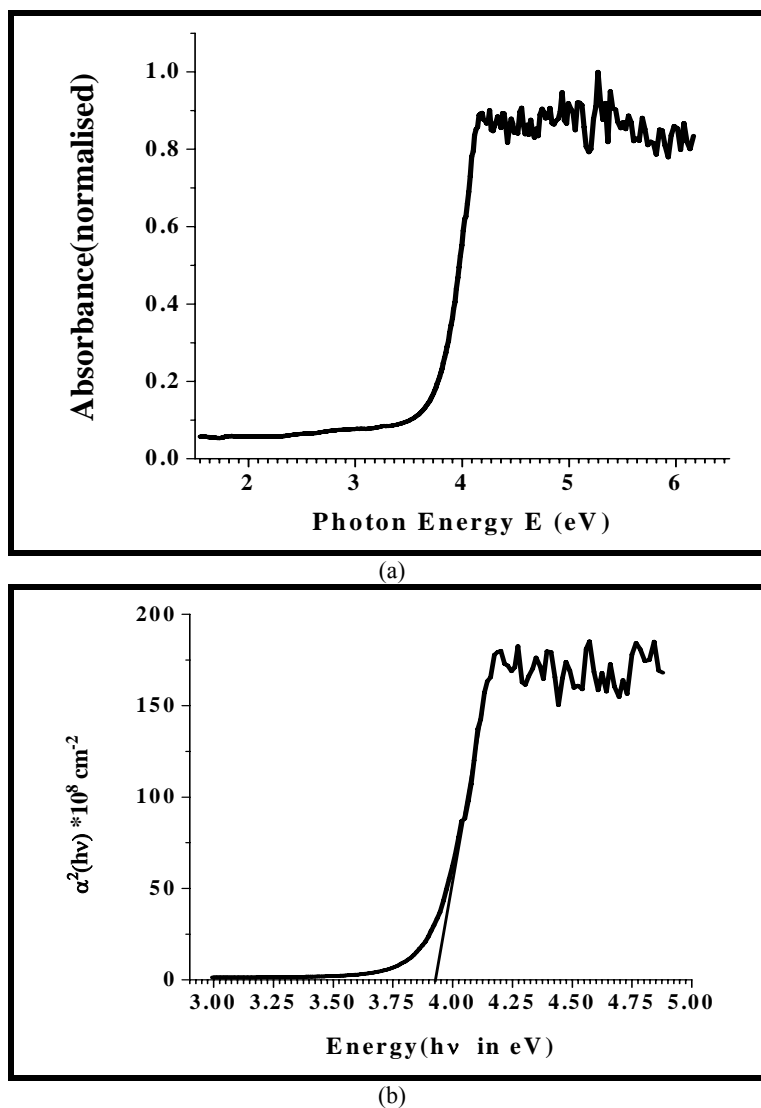


Fig. 4 (a) UV-visible spectra of  $\text{ZnFe}_2\text{O}_4$ , (b) Tauc plot for band gap calculation of zinc ferrite nanocomposite.

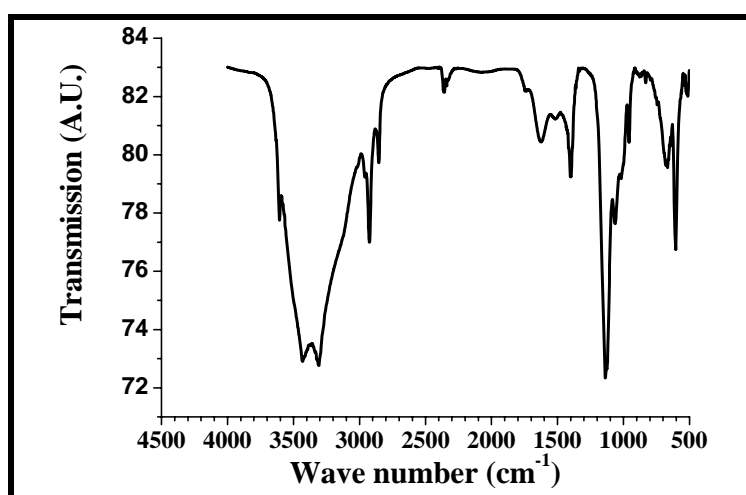


Fig. 5 FTIR spectra of  $\text{ZnFe}_2\text{O}_4$  nanocomposite.

attributed to the stretching vibration mode of M-O for zinc ferrite nanocomposite. The broad band at around  $3,450$  and  $1,634\text{ cm}^{-1}$  correspond to the stretching and bending modes of the OH group of water and Ethylene glycol. The peaks at  $2,927$  and  $2,845\text{ cm}^{-1}$  are assigned to the asymmetric and symmetric methylene stretches ( $-\text{CH}_2$ ) of ethylene glycol. The peak at  $1045\text{ cm}^{-1}$  corresponds to the C-OH stretching vibration of ethylene glycol.

#### 4. Gas Sensing Studies and Discussion

Fig. 6 shows the variations in resistance of mixed shaped zinc ferrite pellet for different vol.% of LPG at room temperature as a function of time. It indicates that as time increases the resistance of sensing pellet increases drastically in the beginning and then increases slowly after that it attains a constant value. Curve '1' of Fig. 5 for 1 vol.% of LPG shows that as time increases the resistance of pellet increases drastically from 1 to  $4.18\text{ M}\Omega$ , after that it increases linearly from  $4.18$  to  $4.38\text{ M}\Omega$  with slow response, further, it becomes constant. Again when we introduced 2 vol.% of LPG, resistance increases drastically from 1 to  $5.35\text{ M}\Omega$ , after that it increases linearly from  $5.35$  to  $5.80\text{ M}\Omega$  which is shown by curve '2'. This curve shows better slope than previous which indicates the slightly improved sensitivity than

previous. Similarly curves '3' and '4' for 3 and 4 vol.% of LPG respectively, show better slope than both the previous and hence successive improvements in their sensitivities. Finally when we introduced 5 vol.% of LPG, resistance increases drastically from 1 to  $6.86\text{ M}\Omega$ , after that it increases slowly and finally becomes constant, which is shown by curve '5'. This is the maximum variation in resistance which gives higher slope and hence highest sensitivity for devising a LPG sensor. A variation of sensor response with time for different LPG concentrations is illustrated in Fig. 7. This figure indicates that as the concentration of LPG increases, the sensor response increases. The low concentration implies a lower surface coverage of gas molecules, resulting in a lower surface reaction between the surface adsorbed oxygen species and the gas molecules. The increase in LPG concentration, increases the surface reaction due to a large surface coverage. Further on increasing the LPG concentration, the surface reaction does not increase and eventually saturation takes place. The maximum sensor response was 496 for 5 vol.% of LPG. High response would be expected if the amount of adsorbed LPG is larger and reaction between the adsorbed LPG and oxygen species is more favorable. Average sensitivity was plotted as a function of concentration of LPG as shown in Fig.8. Reproducibility curve for

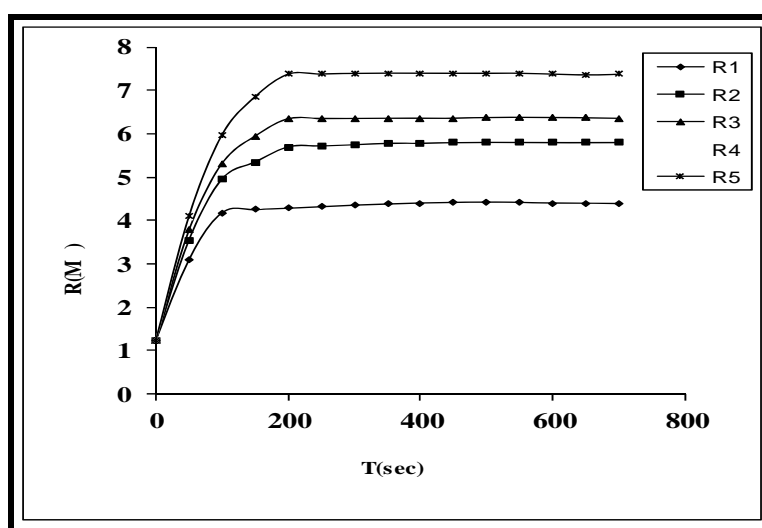


**Fig. 6** Variations of resistance of solid state  $\text{ZnFe}_2\text{O}_4$  pellet with time for different vol.% of LPG.

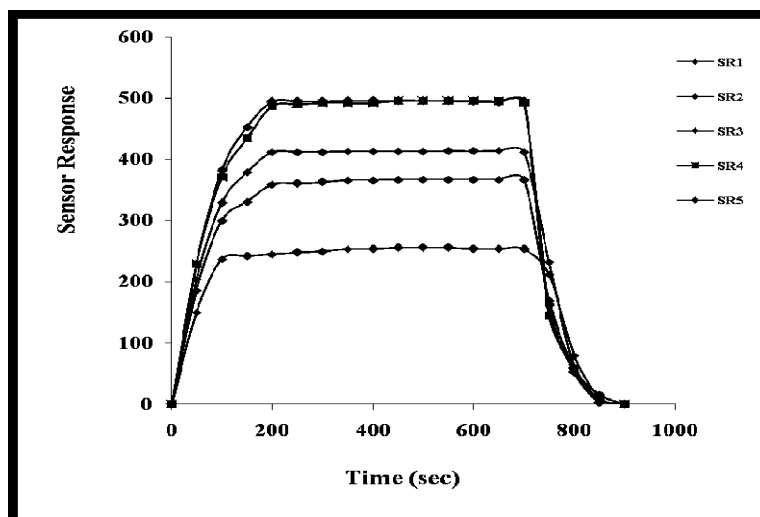


Fig. 7 Sensor Response curves of  $\text{ZnFe}_2\text{O}_4$  sensing material.

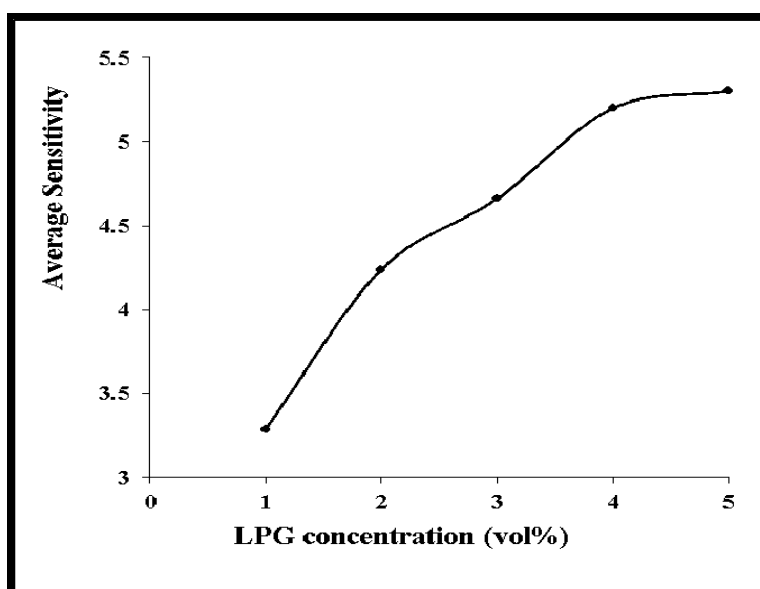


Fig. 8 Variations of average sensitivity with concentration of LPG for  $\text{ZnFe}_2\text{O}_4$  LPG sensor.

this sensor after one month for 5 vol.% of LPG is plotted and shown in Fig. 9. It shows that the sensor is 98% reproducible after one month.

Another important factor for every gas sensor is its response and recovery times, when the sensor is exposed to and then removed from the gas environment. Here, the response time required for the response value to attain 90% of its maximum value is shorter ( $\sim 90$  s) for zinc ferrite pellet. As the LPG gas was turned-off, the response of the same film fell rapidly, indicating that the good recovery of the resistance was obtained for this pellet. The time taken

by the sensor elements to come back once the LPG was removed is found longer ( $\sim 130$  s).

It is well known that the sensitivity of the metal-oxide semiconductor sensors is mainly resolute by the interactions between the target gas molecules and active adsorption surface sites of the sensor. So, it is obvious that for the greater specific surface area of the materials, the interaction between the adsorbed gases and the sensor surface will be stronger, i.e. sensitivity will be higher. LPG is always adsorbed and evenly react with the surface, therefore small particle size and large specific area of zinc ferrite contribute to

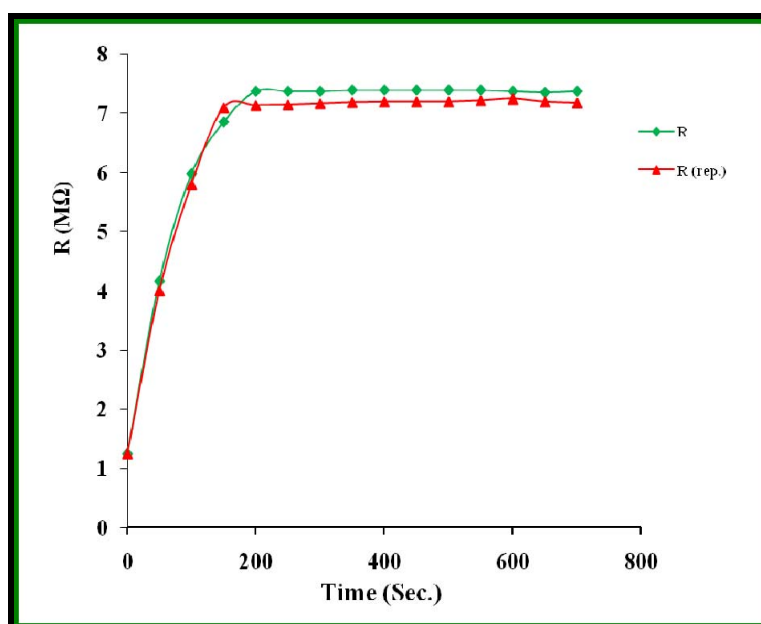


**Fig. 9** Reproducibility curve for the sensing material at 5 vol.% of LPG.

oxygen and LPG adsorption on its sensing surface, which is responsible for the increase in sensitivity of the sensor.

The LPG sensing mechanism is based on the changes in the resistance of the  $\text{ZnFe}_2\text{O}_4$  pellet. The oxygen adsorbed on the surface of the pellet influences the resistance of the  $\text{ZnFe}_2\text{O}_4$  based sensor. Initially oxygen from the atmosphere adsorbs on the surface of the pellet and extracts electrons from its conduction bands to form  $\text{O}_2^-$  species on the surface, consequently resistance increases. After that an equilibrium state is achieved between oxygen of  $\text{ZnFe}_2\text{O}_4$  and atmospheric oxygen and the value of stabilized resistance was recorded. When the pellet is exposed to LPG, it reacts with the chemisorbed oxygen. On interaction with hydrocarbons ( $\text{C}_n\text{H}_{2n+2}$ ) of LPG the adsorbed oxygen is removed, forming gaseous species and water vapor. Consequently, the resistance changes, which is due to the change in the width of depletion layer after exposure to LPG.

When the LPG reacts with the surface oxygen ions then the combustion products such as water depart and a potential barrier to charge transport would be developed i.e., this mechanism involves the displacement of adsorbed oxygen species by

formation of water. The formation of barrier is due to reduction in the concentration of conduction carriers and thereby, results in an increase in resistance of the sensing element with time. As the pressure of the gas inside the chamber increases, the rate of the formation of such product increases and potential barrier to charge transport becomes strong which has stopped the further formation of water constituting the resistance constant.

Table 1 presents the comparison of LPG response between earlier reported LPG sensors by our group and synthesized  $\text{ZnFe}_2\text{O}_4$  nanoparticles in the present investigation. It is clear that response of sensor reported in this paper is higher as compared to reported sensors. Thus our investigation show significant advancement towards the fabrication of a reliable and cost effective LPG sensor operable at room temperature.

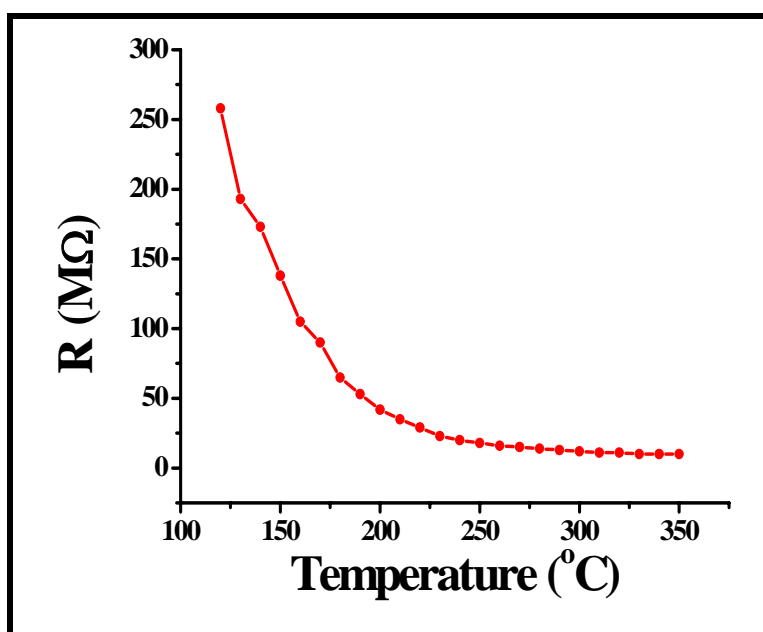
## 5. Electrical Measurements and Discussion

Fig. 10 shows the variations in electrical resistance of  $\text{ZnFe}_2\text{O}_4$  in the temperature range 125-350 °C in air. Initially, the resistance of sensors decreases sharply with temperature. It appears to follow the exponent law approximately. This is due to the ionization of



**Table 1**

S. No.	Sensing material	Sensor response (%)	Response time (s)	Recovery time (s)	Reference No.
1.	Zinc oxide	11	-	-	21
2	Zinc niobate	12	120	290	22
3	Titanium oxide	45	130	300	11
4	Ferric oxide	213	150	280	10
5	Cobalt zincate	342	320	460	23
6	Zinc oxide	396	90	120	7
7	Zinc ferrite nanorods	140	60	300	24
8	Zinc Ferrite	496	70	130	Present work



**Fig. 10** Variations in resistance of the sensing element with the temperature in air.

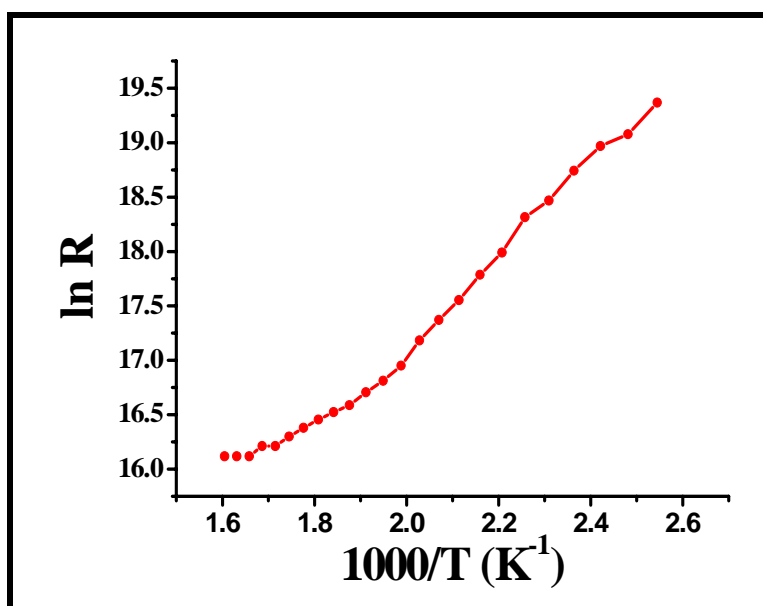
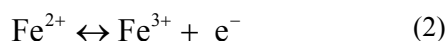


**Fig. 11** Arrhenius plot for the sensing element ZnFe<sub>2</sub>O<sub>4</sub>.

donor impurity and defects. Finally, the change in resistance is small. It is because the electrons of donor level are ionized completely, and the electronic concentration of intrinsic excitation is lesser than the concentration of donor at this temperature region with increasing temperature. The resistance decreases as per exponent's law because of increasing of electronic concentration that is rooted in the process of intrinsic excitations. The decrease in resistance with increasing temperature is related to an increase in drift mobility of the thermally activated electrons according to the hopping conduction mechanism. The valence exchange:



which is the main source of electron hopping in this process. The electrical conduction in zinc ferrite is attributed to electron hopping between the two valence state of iron, Fe<sup>2+</sup> and Fe<sup>3+</sup> on the octahedral sites in the spinel lattice [20]. The characteristics of a semiconducting gas sensor have a major dependence on two factors. One is the intrinsic conduction mechanism and the other is the pore size and distribution. Both factors influence the kinetics of the chemisorption reaction between the sensor and the surrounding gases. Fig. 11 shows an Arrhenius plot of the temperature dependence electrical resistance of ZnFe<sub>2</sub>O<sub>4</sub> in air. The logarithm of resistance of ZnFe<sub>2</sub>O<sub>4</sub> had an almost linear relationship with reciprocal temperature (1/T) as expected for a typical semiconducting material. Arrhenius plot has a slope (E<sub>a</sub>/2K) according to equation:

$$\ln R = \ln R_0 + E_a / 2KT \quad (3)$$

where, E<sub>a</sub>, K and T are the activation energy, Boltzmann constant and absolute temperature of the material, respectively. The activation energy (E<sub>a</sub>) determined in terms of the slope of the Arrhenius plot was found 0.56 eV. The extent of adsorbed oxygen ions and existence of their different chemical forms (O<sub>2</sub>, O<sub>2</sub><sup>-</sup>, O<sup>-</sup> or O<sup>2-</sup>) on the sensor surface are controlled by the sensor operating temperature. It can

be noted that a change in temperature will alter the resistance because both the charge of the surface species as well as their coverage can be altered in this process. As the interaction probability of sensing element with LPG is given by the Boltzmann factor exp(-E<sub>a</sub>/kT). Therefore for the higher probability of interaction to be occurring, E<sub>a</sub> should be least for room temperature LPG sensors. Thus, this small value of activation energy of sensing film is significant for the detection of LPG at room temperature.

## 6. Conclusions

Zinc ferrite was successfully synthesized via co-precipitation method and characterized for their structural and surface morphological properties. From SEM images we observed that there were spherical zinc ferrite nanoparticles, few particles agglomerated and leaving vacant spaces among them. The XRD patterns show nanocrystalline nature of the materials with spinel phase. The minimum crystallite size of zinc ferrite was found 8 nm. Appreciable changes in resistance of nano sized ZnFe<sub>2</sub>O<sub>4</sub> upon exposure to LPG in ambient atmosphere recognized zinc ferrite as a LPG sensor. The maximum sensor response obtained with ZnFe<sub>2</sub>O<sub>4</sub> to LPG was 496. Thus, the present study explored the possibility of making use of ZnFe<sub>2</sub>O<sub>4</sub> for LPG sensing at room temperature.

## References

- [1] Reddy, C. V. G., Manorama, S. V. and Rao, V. J. 2000. "Preparation and Characterization of Ferrites as Gas Sensor Materials." *Journal of Material Science Letters* 19: 775-8.
- [2] Jiao, Z., Wu, M. H., Gu, J. Z. and Qin, Z. 2003. "Preparation and Gas-Sensing Characteristics of Nanocrystalline Spinel Zinc Ferrite Thin Films." *IEEE Sensors Journal* 3: 435-8.
- [3] Bharti, D. C., Mukherjee, K. and Majumder, S. B. 2010. "Wet Chemical Synthesis and Gas Sensing Properties of Magnesium Zinc Ferrite Nano-Particles." *Material Chemistry Physics* 120: 509-17.
- [4] Mukherjee, K. and Majumder, S. B. 2010. "Reducing Gas Sensing Behaviour of Nanocrystalline Magnesium Zinc Ferrite Powders." *Talanta* 81: 1826-32.

- [5] Arshak, K. and Gaidan, I. 2005. "Development of a Novel Gas Sensor Based on Oxide Thick Films." *Materials Science and Engineering B* 118: 44-9.
- [6] Lee, G. G. and Kang, S. J. L. 2005. "Formation of Large Pores and Their Effect on Electrical Properties of SnO<sub>2</sub> Gas Sensors." *Sensors and Actuators B* 107: 392-6.
- [7] Yadav, A. and Yadav, B. C. 2012. "A Mechanochemical Synthesis of Nanostructured Zinc Oxide via Acetate Route for LPG Sensing." *Journal of Experimental Nanoscience* 5: 1-11.
- [8] Khadayate, R. S., Sali, J. V., Rane, S. B. and Patil, P. P. 2007. "Preparation and Characterization of WO<sub>3</sub>-Based Liquid Petroleum Gas Sensor." *Materials and Manufacturing Processes* 22: 277-80.
- [9] Yadav, B. C., Singh, S. and Yadav, A. 2011. "Nanonails Structured Ferric Oxide Thick Film as Room Temperature Liquefied Petroleum Gas (LPG) Sensor." *Applied Surface Science* 257: 1960-6.
- [10] Yadav, B. C., Singh, S., Yadav, A. and Shukla, T. 2011. "Experimental Investigations on Nano-Sized Ferric Oxide and Its LPG Sensing." *Int. Journal of Nanoscience* 10: 1-5.
- [11] Yadav, B. C., Yadav, A., Shukla, T. and Singh, S. 2011. "Solid State Titania Based Gas Sensor for Liquefied Petroleum Gas Detection at Room Temperature." *Bulletin of Materials Science* 34: 1639-44.
- [12] Bangale, S. V., Patil, D. R., and Bamane, S. R. 2011. "Nanostructured Spinel ZnFe<sub>2</sub>O<sub>4</sub> for the Detection of Chlorine Gas." *Sensors and Transducers Journal* 134: 107-19.
- [13] Carotta, M. C., Martinelli, G., Sadaoka, Y., Nunziante, P. and Traversa, E. 1998. "Gas Sensitive Electrical Properties of Perovskite-Type SmFeO<sub>3</sub> Thick Films." *Sensor and Actuators B* 48: 270-6.
- [14] Chu, X. F., Liu, X. Q. and Meng, G. Y. 1999. "Preparation and Gas Sensitivity Properties of ZnFe<sub>2</sub>O<sub>4</sub> Semiconductors." *Sensor and Actuators B* 55: 19-22.
- [15] Bangale, S. V. and Bamane, S. R. 2012. "Preparation and Study of H<sub>2</sub>S Gas Sensing Behaviour of ZnFe<sub>2</sub>O<sub>4</sub> Thick Film Resistors." *Sensors and Transducers Journal* 137: 123-36.
- [16] Mukherjee, K. and Majumder, S. B. 2010. "Analyses of Conductance Transients to Address the Selectivity, Issue of Zinc Ferrite Gas Sensors." *Electrochemical Solid-State Letters* 13 :J25-J27.
- [17] Niu, X. L., Du, W. P. and Du, W. M. 2004. "Preparation and Gas Sensing Properties of ZnM<sub>2</sub>O<sub>4</sub> (M = Fe, Co, Cr)." *Sensors and Actuators B* 99: 405-9.
- [18] Chu, X. F., Liu, X. Q., and Meng, G. Y. 2000. "Effects of CdO Dopant on the Gas Sensitivity Properties of ZnFe<sub>2</sub>O<sub>4</sub> Semiconductors." *Sensors and Actuators B* 65: 64-7.
- [19] Arshak, K. and Gaidan, I. 2005. "Gas Sensing Properties of ZnFe<sub>2</sub>O<sub>4</sub>/ZnO Screen-Printed Thick Films." *Sensors and Actuators B* 111: 58-62.
- [20] Smit, J. and Wijn, H. P. J. 1961. *Les Ferrites*, Dunod, Paris.
- [21] Yadav, B. C., Srivastava, R. and Yadav, A. 2009. "Nanostructured Zinc Oxide Synthesized via Hydroxide Route as Liquid Petroleum Gas Sensor." *Sensor and Materials* 21: 87-94.
- [22] Yadav, B. C., Yadav, A., Shukla, T. and Singh, S. 2009. "Experimental Investigations on Solid State Conductivity of Cobaltzincate Nanocomposite for Liquefied Petroleum Gas Sensing." *Sensor letters* 7: 1119-23.
- [23] Yadav, B. C., Srivastava, R., Yadav, A. and Srivastava, V. 2008. "LPG Sensing of Nanostructured Zinc Oxide and Zinc Niobate." *Sensor letters* 6 :714-8.
- [24] Singh, A., Singh, A., Singh, S., Tandon, P., Yadav, B. C. and Yadav, R. R. 2015. "Synthesis, Characterization and Performance of Zinc Ferrite Nanorods for Room Temperature Sensing Applications." *Journal of Alloys and Compounds* 618: 475-83.